Auditory midbrain representation of a break in interaural correlation

Qian Wang[1] and Liang Li[1,2,3,4]

[1]*Department of Psychology and Beijing Key Laboratory of Behavior and Mental Health, Peking University, Beijing, People's Republic of China;* [2]*Speech and Hearing Research Center, Key Laboratory on Machine Perception (Ministry of Education), Peking University, Beijing, People's Republic of China;* [3]*PKU-IDG/McGovern Institute for Brain Research, Peking University, Beijing, People's Republic of China; and* [4]*Beijing Institute for Brain Disorders, Beijing, People's Republic of China*

Wang Q, Li L. Auditory midbrain representation of a break in interaural correlation. *J Neurophysiol* 114: 2258–2264, 2015. First published August 12, 2015; doi:10.1152/jn.00645.2015.—The auditory peripheral system filters broadband sounds into narrowband waves and decomposes narrowband waves into quickly varying temporal fine structures (TFSs) and slowly varying envelopes. When a noise is presented binaurally (with the interaural correlation being 1), human listeners can detect a transient break in interaural correlation (BIC), which does not alter monaural inputs substantially. The central correlates of BIC are unknown. This study examined whether phase locking-based frequency-following responses (FFRs) of neuron populations in the rat auditory midbrain [inferior colliculus (IC)] to interaurally correlated steady-state narrowband noises are modulated by introduction of a BIC. The results showed that the noise-induced FFR exhibited both a TFS component (FFR_{TFS}) and an envelope component (FFR_{Env}), signaling the center frequency and bandwidth, respectively. Introduction of either a BIC or an interaurally correlated amplitude gap (which had the summated amplitude matched to the BIC) significantly reduced both FFR_{TFS} and FFR_{Env}. However, the BIC-induced FFR_{TFS} reduction and FFR_{Env} reduction were not correlated with the amplitude gap-induced FFR_{TFS} reduction and FFR_{Env} reduction, respectively. Thus, although introduction of a BIC does not affect monaural inputs, it causes a temporary reduction in sustained responses of IC neuron populations to the noise. This BIC-induced FFR reduction is not based on a simple linear summation of noise signals.

envelope; frequency-following responses; inferior colliculus; interaural correlation; temporal fine structure

INTERAURAL CORRELATION (IAC) is defined as the similarity of sound waves presented at the two ears (Jeffress et al. 1962). IAC-based binaural processing plays a critical role in both sound localization (Coffey et al. 2006; Franken et al. 2014; Soeta and Nakagawa 2006) and target-object detection in noisy environments (Durlach et al. 1986; Palmer et al. 1999). The IAC also affects the auditory perception. For example, when the IAC drops from 1 to 0, without affecting the spectra of monaural inputs, the auditory image of the simultaneously arriving binaural sounds changes vividly from a single image located at the head center into two separated images at each ear (Blauert and Lindemann 1986; Culling et al. 2001). Accordingly, human listeners with normal hearing can easily detect an interaurally uncorrelated fragment embedded in the interaurally correlated noises (Akeroyd and Summerfield 1999; Boehnke et al. 2002; Huang et al. 2008, 2009a, 2009b; Kong et

al. 2012, 2015; Li et al. 2009, 2013), i.e., a transient change of IAC from 1 to 0, then back to 1 [so-called "break in interaural correlation" (BIC)]. Note that introduction of a BIC does not significantly alter monaural inputs. Until now, the neural correlates of the BIC in the central auditory system have not been reported in the literature.

The peripheral auditory system not only band-pass filters broadband sounds into a series of narrowband waves orderly distributing along the basilar membrane but also decomposes narrowband waves into both quickly varying temporal fine structures (TFSs) and slowly varying envelopes (Moore 2008; Rosen 1992). These two temporal components are subsequently represented by temporal firing patterns of the auditory nerves (Johnson 1980; Joris and Yin 1992; Young and Sachs 1979). Although the neural representation of a BIC in the central auditory system may contain TFS and envelope components, listeners in fact do not perceive the BIC as separated TFS and envelope percepts.

Both scalp-recorded and intracranially recorded frequency-following responses (FFRs) are sustained neuroelectrical potentials based on precisely phase-locked responses of neuron populations to instantaneous waveforms of low- to middle-frequency acoustic stimuli (Chandrasekaran and Kraus 2010; Du et al. 2009a, 2009b, 2011, 2012; Marsh and Worden 1969; Moushegian et al. 1973; Ping et al. 2008; Weinberger et al. 1970; Worden and Marsh 1968). FFRs can efficiently convey both TFS information (e.g., Chandrasekaran and Kraus 2010; Du et al. 2011; Galbraith 1994; Krishnan 2002; Krishnan and Gandour 2009; Russo et al. 2004) and envelope information (also called envelope-following response) (e.g., Aiken and Picton 2006, 2008; Dolphin and Mountain 1992, 1993; Hall 1979; Shinn-Cunningham et al. 2013; Supin and Popov 1995; Zhu et al. 2013). FFRs start to occur in the auditory nerve (Dau 2003) and can be intracranially recorded in both the lower auditory brain stem structures (Kuokkanen et al. 2010; Wagner et al. 2005, 2009) and the auditory midbrain, the inferior colliculus (IC) (Du et al. 2009b; Ping et al. 2008). In humans, the origin of human scalp-recorded FFRs has been widely considered to be the IC (e.g., Chandrasekaran and Kraus 2010; Marsh 1974; Smith et al. 1975; Sohmer et al. 1977; Weinberger et al. 1970).

The IC is the end point that both converges inputs from lower auditory brain stem structures and processes IAC signals (Palmer et al. 1999; Shackleton et al. 2005; Shackleton and Palmer 2006; Yin et al. 1987). It is also considered the critical generator for human scalp-recorded FFRs (Chandrasekaran and Kraus 2010; Marsh 1974; Smith et al. 1975; Sohmer et

1977; Weinberger et al. 1970). This study investigated the following four issues with rats as the mammal modeling subjects: *1*) in the IC, whether a narrowband noise can evoke local-field FFRs that contain the TFS component (FFR$_{TFS}$) and the envelope component (FFR$_{Env}$); *2*) whether the FFR$_{TFS}$ and/or FFR$_{Env}$ to interaurally correlated noises are affected by introduction of a BIC; *3*) whether the BIC-evoked change in FFR$_{TFS}$ contributes to the neural BIC detection differently from that in FFR$_{Env}$; and *4*) whether the binaural integration of IC neuron populations for neural detection of a BIC is based on a simple linear summation (i.e., cross-correlation) of noise signals from the two ears.

MATERIALS AND METHODS

Animal preparation. Eight young adult male Sprague-Dawley rats (age 10–12 wk, weight 280–350 g) were purchased from the Vital River Experimental Animal Company. They were anesthetized with 10% chloral hydrate (400 mg/kg ip), and the state of anesthesia was maintained throughout the experiment by supplemental injection of the same anesthetic. Stainless steel recording electrodes (10–20 kΩ) insulated by a silicon tube (0.3 mm in diameter) except at the 0.25-mm-diameter tip (Du et al. 2009b; Ping et al. 2008) were aimed at the central nucleus of the IC bilaterally. Based on the stereotaxic coordinates of Paxinos and Watson (1997) and referenced to bregma, the coordinates of the aimed IC site were AP, −8.8 mm; ML, ±1.5 mm; DV, −4.5 to −5.0 mm. Two electrodes were inserted per animal, one on each side of the IC.

Rats used in this study were treated in accordance with the Guidelines of the Beijing Laboratory Animal Center and the *Policies on the Use of Animals and Humans in Research* approved by the Society for Neuroscience (2006). The experimental procedures were also approved by the Committee for Protecting Human and Animal Subjects in the Department of Psychology at Peking University.

Apparatus and stimuli. All sound waves were processed by a TDT System II (Tucker-Davis Technologies) and presented through two ED1 earphones. Two 12-cm TDT sound-delivery rubber tubes were connected to the ED1 earphones and inserted into each of the rat's ear canals for sound delivery. All narrowband noises were calibrated with a Larson Davis Audiometer Calibration and Electroacoustic Testing System (AUDit and System 824, Larson Davis). The sound pressure level (SPL) of all signals was 72 dB for each earphone.

Gaussian wideband noises (10-kHz sampling rate and 16-bit amplitude quantization) were generated and filtered by a 512-point digital filter with a center frequency of 2,000 Hz and a bandwidth of 0.466 octaves with MATLAB (MathWorks, Natick, MA). The stimulus duration was 900 ms with 10-ms linear onset/offset ramps, and the (offset-onset) interstimulus interval was 100 ms.

Under the baseline-stimulation condition that occurred before and after the occurrence of either the BIC or the interaurally correlated amplitude gap (Corgap), the interaurally correlated noises (IAC = 1) were presented for the total duration of 900 ms. Under the BIC-stimulation condition, a 200-ms uncorrelated noise fragment (IAC = −0.046) was substituted into the temporal middle of the noise (i.e., from 350 to 550 ms from the noise onset) with no interaural delays. Note that mathematically the amplitude of the linear summation of two uncorrelated noises is smaller than that of two correlated noises (Fig. 1). Thus if the central binaural integration follows the simple theoretical summation, the magnitude of neural signals under the BIC-stimulation condition should be smaller than that under the baseline-stimulation condition (Fig. 1*B*, *left*).

Since the linear summation of binaural signals under the BIC-stimulation condition leads to an amplitude reduction (Fig. 1*A*), the Corgap-stimulation condition was introduced as the stimulation control condition. Under the Corgap-stimulation condition, the two monaurally presented noises were identical (correlated), but their ampli-

tudes were equal to 50% of the left-right summated signal amplitude under the BIC-stimulation condition. In other words, the linearly summated left ear and right ear signals under the BIC-stimulation condition and those under the Corgap-stimulation condition are identical (Fig. 1). The BIC and Corgap were distinguished in the value of the IAC coefficient (during the fragment period from 350 to 550 ms after the sound onset). Note that monaurally the intensity of the Corgap-stimulation condition was reduced during the fragment period compared with the pre- and postfragment periods but the monaural intensity under the BIC-stimulation condition was not reduced.

Evoked neural potentials were recorded in a sound-attenuating chamber, amplified 1,000 times by a TDT DB4 amplifier, filtered through a 100- to 10,000-Hz band-pass filter (with a 50-Hz notch), and averaged 100 times per stimulation condition. Online recordings were processed with TDT Biosig software, digitized at 16 kHz, and stored on a disk for off-line analyses. The same stimuli were used for each animal under a certain stimulation condition. Also, both the prefragment and the postfragment were not changed across stimulation conditions.

Data analyses. Theoretically, a steady-state Gaussian narrowband noise with a center frequency of *c* Hz and a bandwidth of *b* Hz has a TFS energy around *c* Hz and an envelope energy within the frequency range between 0 and *b* Hz (Longtin et al. 2008). Thus for a narrowband noise with bandwidth *b*, the TFS energy distributes from the low-cut (f_{lc}) to the high-cut (f_{hc}) frequencies, and the f_{hc} is below the frequency *b*. The normalized amplitude of FFR$_{TFS}$ can be calculated by the following function:

$$\text{FFR}_{\text{TFS}}\_\text{normalized}\_\text{amplitude} = \sum_{l=f_{lc}}^{f_{hc}} \text{Amp}_l \left/ \sum_{n=2}^{5,000} \text{Amp}_n \right. \quad (1)$$

The normalized amplitude of FFR$_{Env}$ can be calculated by the following function:

$$\text{FFR}_{\text{Env}}\_\text{normalized}\_\text{amplitude} = \sum_{l=2}^{b} \text{Amp}_l \left/ \sum_{n=2}^{5,000} \text{Amp}_n \right. \quad (2)$$

where the denominator represents the level of noise floor ranging from 2 to 5,000 Hz while the numerator represents the spectral region of interest. The FFR$_{TFS}$ and FFR$_{Env}$ components were extracted to calculated normalized amplitude with *functions 1* and *2*.

To estimate the neural detection of the BIC fragment and that of the Corgap fragment, responses in each of the three 200-ms periods were separately processed: prefragment (100–300 ms after noise onset), fragment (350–550 ms), and postfragment (600–800 ms). Furthermore, the (neural) fragment detection index (FDI) was defined as the relative difference between the amplitude of the fragment (BIC or Corgap) and the average of prefragment amplitude and postfragment amplitude (normalized against the average of pre- and postfragment amplitudes).

Statistical analyses. Statistical analyses were performed with IBM SPSS Statistics 20 (SPSS, Chicago, IL). Within-subjects, repeated-measures analyses of variance (ANOVAs), *t*-tests, and Pearson correlation were conducted to examine differences between stimulation conditions or correlation between responses. The null hypothesis rejection level was set at 0.05.

Histology. When all recordings were completed, rats were euthanized with an overdose of chloral hydrate. Lesion marks were made via the recording electrodes with an anodal DC current (500 μA for 10 s). The brains were stored in 10% formalin with 30% sucrose and then sectioned at 55 μm in the frontal plane in a cryostat (−20°C). Sections were examined to determine locations of recording electrodes.
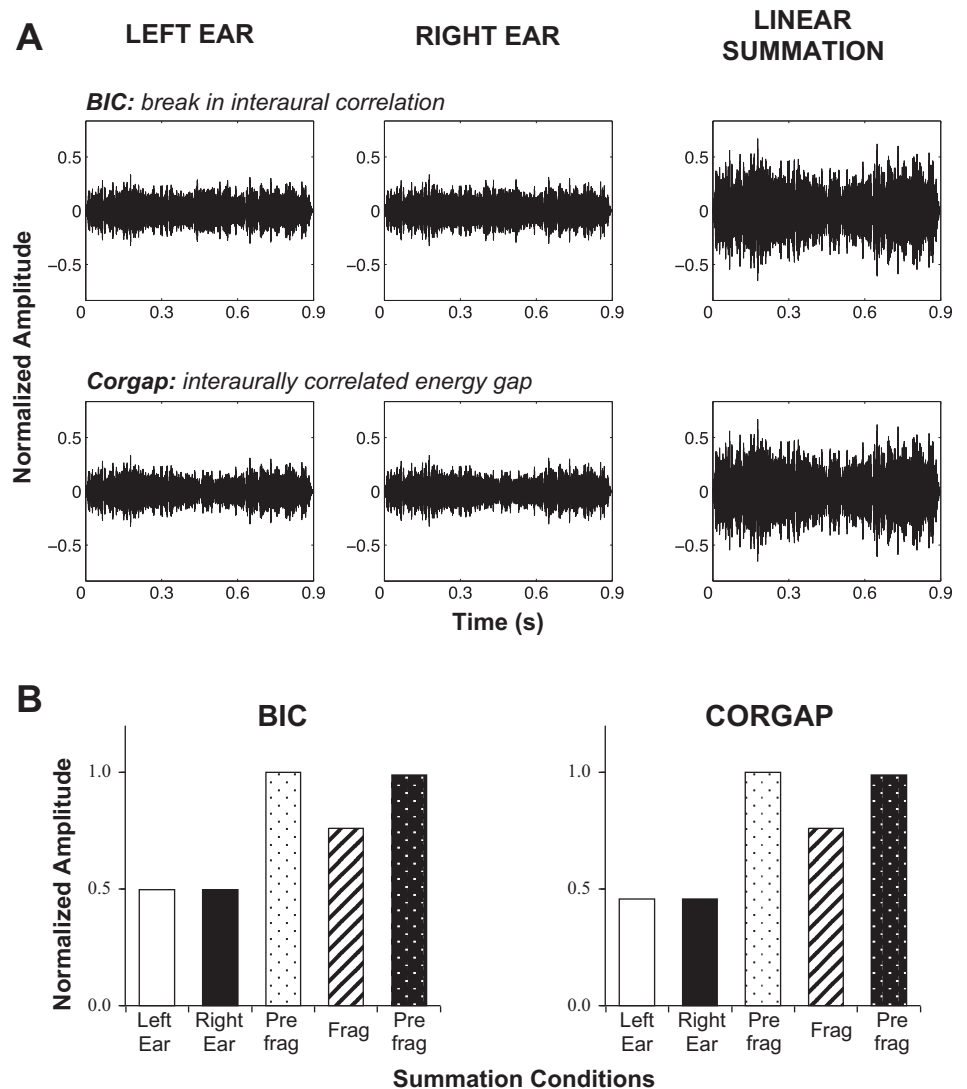
Fig. 1. *A*: waveforms of the monaural noise stimuli and the theoretically linearly summated waveforms of the monaural stimuli. Under the condition of break in interaural correlation (BIC), a 200-ms uncorrelated noise pair was substituted into the temporal middle (350–550 ms from the onset) of the noise stimuli. Under the condition of interaurally correlated amplitude gap (Corgap), the two monaurally presented noises were identical (correlated) but their amplitudes were individually equal to 50% of the left-right summated signal amplitude under the BIC-stimulation condition. *B*: comparisons in normalized amplitude between the baseline-stimulation condition (pre- and postfragment), the BIC-stimulation condition, and the Corgap-stimulation condition. Note that under the Corgap-stimulation condition the amplitude of the noise at each ear was so reduced that the linear summation of the noises from the 2 ears led to a noise signal identical to that after the linear summation of the noises from the 2 ears under the BIC-stimulation condition.

RESULTS

Histological results and response latencies. According to the histological examination, all 16 electrodes were located precisely within the central nucleus of IC in all rats (Fig. 2*A*). Each of the electrodes was used in experimental recordings. The response latency to the noise stimulus onset was examined by cross-correlation analyses of the best delay between the noise stimulus waveform and the evoked neural response waveform (Burkard 1991; Dobie and Wilson 1984). The best delay, at which the stimulus-response correlation reached the maximum, ranged from 5.8 to 6.1 ms with a mean of 6.0 ms, consistent with the results reported by previous studies (Du et al. 2011; Ping et al. 2008).

To estimate whether binaural sluggishness exists in IC FFRs, the latency of IC FFR to the BIC was compared to that to the Corgap by cross-correlation analyses of the best delay between the fragment waveform (350–550 ms after sound onset) and the evoked neural response waveform. Pairwise *t*-test showed that there was no significant difference between the latency for BIC (mean = 5.99, SD = 0.35) and that for Corgap (mean = 6.01, SD = 0.39) [$t(13) = -0.034$, $P =$

0.974]. The results suggested that there was no binaural sluggishness at the midbrain level (also see Fitzpatrick et al. 2009).

Effects of BIC or Corgap on FFR_{TFS} and FFR_{Env}. The results of this study clearly showed that narrowband noises could evoke FFRs containing both the FFR_{TFS} and FFR_{Env} components under each of the stimulation conditions (baseline, BIC, and Corgap; see Fig. 2*B* for examples of BIC- and Corgap-stimulation conditions).

The narrowband noise used in this study had a TFS energy around 2,000 Hz (center frequency) and an envelope energy within the frequency range between 0 and 640 Hz (bandwidth). As shown in the example in Fig. 2*B*, *bottom*, the fragment-induced FFR_{TFS} and FFR_{Env} exhibited similar spectra with the stimulus TFS and envelope, respectively (see Longtin et al. 2008).

To examine how faithful the FFR_{TFS} and FFR_{Env} were in representing acoustic features of the noise stimulus, the significance of the stimulus-to-response (S-R) correlation for the prefragment noise section (100–300 ms after sound onset) was examined at each recording site with Pearson correlation tests. The results showed that the S-R correlation between the noise stimulus TFS and the IC FFR_{TFS} was significant (for all
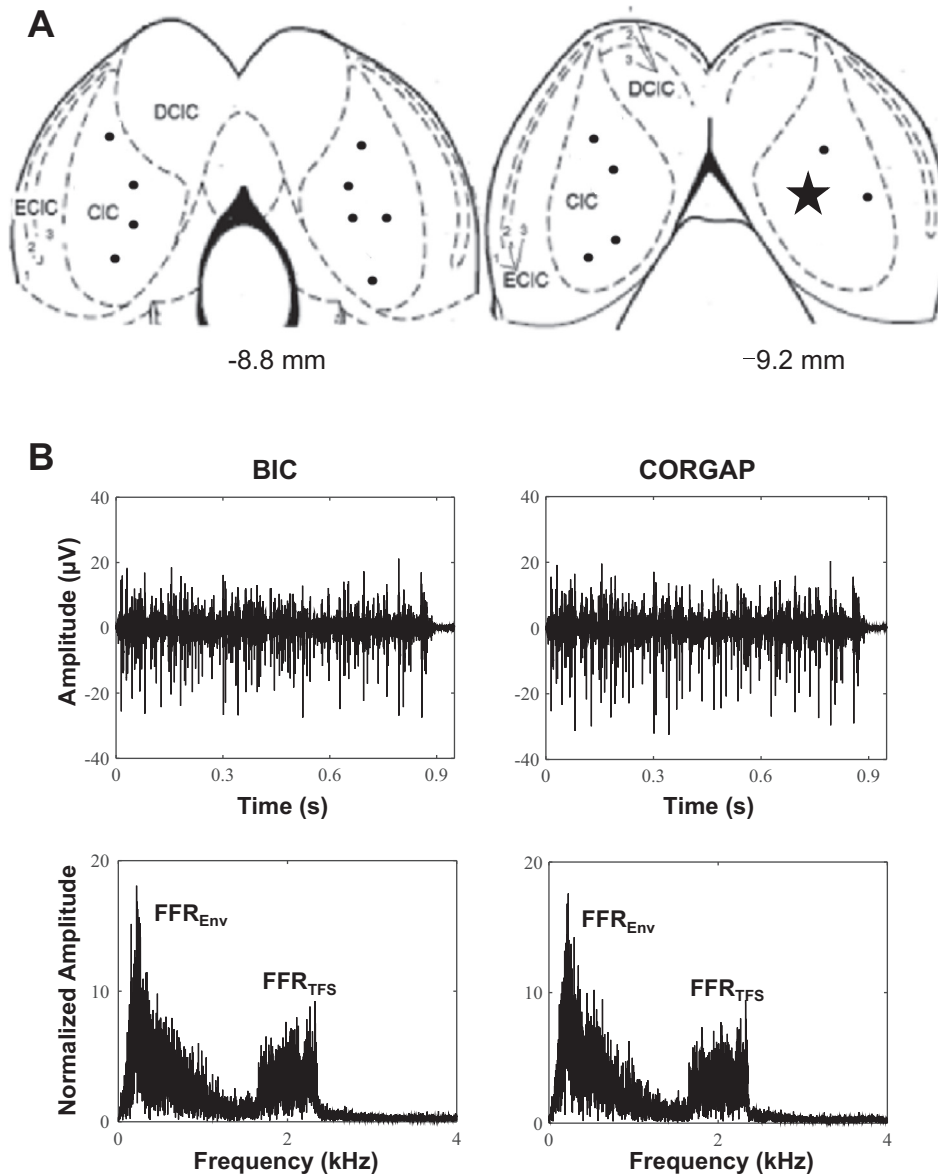
Fig. 2. *A*: histological results of recording electrodes in 8 rats. Electrodes were precisely located within the central nucleus (CIC) of the inferior colliculus (IC) in 16 of the 16 penetrations (filled circles and star). Note that 2 electrodes were inserted per animal, 1 on each side of the IC. DCIC, dorsal cortex of IC; ECIC, external cortex of IC. *B*: frequency-following responses (FFRs) recorded from a randomly selected recording site (star in *A*) to the BIC (*left*) or the Corgap (*right*). The FFRs contained 2 components (FFR_{TFS} and FFR_{Env}) signaling the stimulus temporal fine structure (TFS) and envelope, respectively.

recording sites, $P < 0.05$); the S-R correlation between the noise envelope and the IC FFR_{Env} was also significant (for all recording sites, $P < 0.001$).

To examine whether the BIC and Corgap fragments affected IC FFRs, normalized amplitudes of FFR_{TFS} and FFR_{Env} in the three periods (prefragment, fragment, and postfragment) were calculated separately. Figure 3*A* shows that both FFR_{TFS} and FFR_{Env} decreased as either the BIC or the Corgap occurred. For the FFR_{TFS}, a 2 × 3 (stimulation condition: BIC, Corgap; response period: prefragment, fragment, and postfragment) two-way repeated-measures ANOVA showed that the both the main effect of stimulation condition ($F_{1,15} = 8.889$, $P = 0.009$, partial $\eta^2 = 0.372$) and the main effect of response period ($F_{1,15} = 22.249$, $P < 0.001$, partial $\eta^2 = 0.597$) were significant but the interaction effect was not significant ($F_{2,30} = 0.606$, $P = 0.552$, partial $\eta^2 = 0.039$). Post hoc tests confirmed that the amplitude of FFR_{TFS} during the BIC was significantly lower than that during the Corgap ($P = 0.031$, with Bonferroni adjustment).

For FFR_{Env}, a two-way repeated-measures ANOVA showed that both the main effect of stimulation condition ($F_{1,15} = 5.563$, $P = 0.032$, partial $\eta^2 = 0.271$) and the main effect of response period ($F_{1,15} = 17.629$, $P < 0.001$, partial $\eta^2 = 0.540$) were significant but the interaction between the two factors was not significant ($F_{2,30} = 2.122$, $P = 0.137$, partial $\eta^2 = 0.124$). Post hoc tests confirmed that the amplitude of FFR_{Env} during the BIC was significantly lower than that during the Corgap ($P = 0.040$, with Bonferroni adjustment).

Post hoc tests also showed that no significant differences occurred between the pre- and postfragments under each of the stimulation conditions (for all $P > 0.05$, with Bonferroni adjustment). Thus the normalized amplitudes of pre- and postfragments were averaged in the following analyses of the fragment effects.

Correlations between fragment detection indexes. The FDI was introduced as the relative amplitude difference between FFRs during the fragment and the average of pre- and postfragment FFRs (for details see MATERIALS AND METHODS).
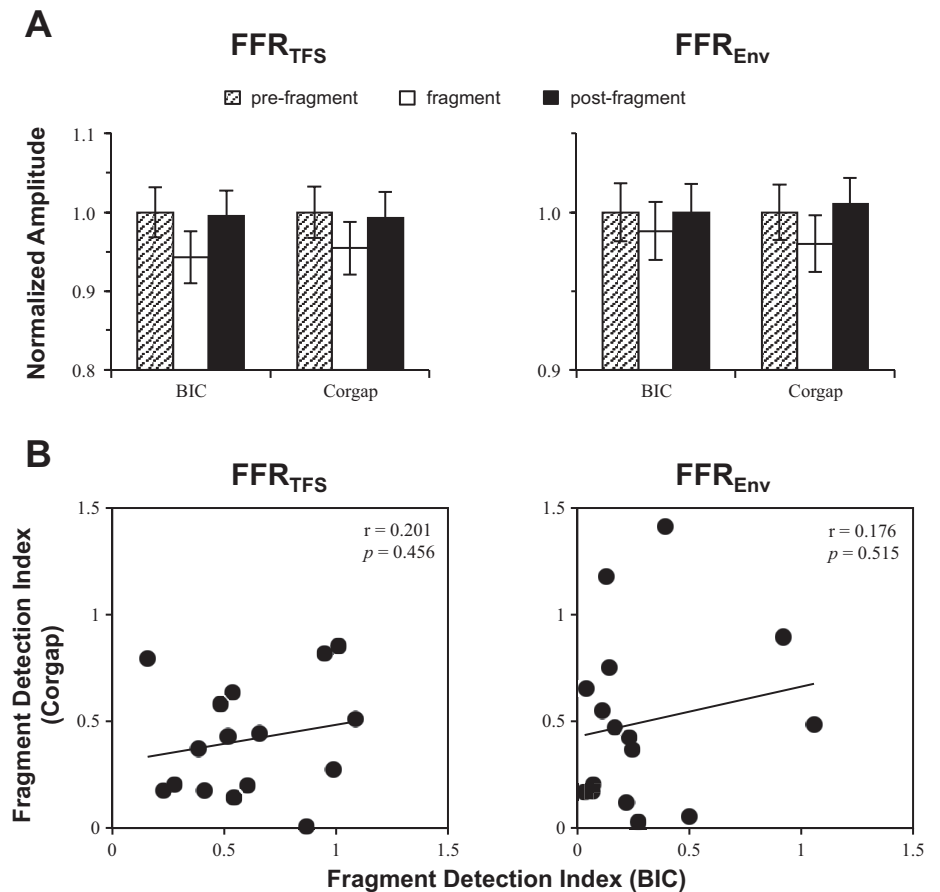
A

Fig. 3. *A*: comparisons in normalized FFR amplitude across stimulation conditions for the FFR_{TFS} (*left*) and the FFR_{Env} (*right*). Fragment period, 350–550 ms after sound onset; prefragment period, 100–300 ms after sound onset; postfragment period, 600–800 ms after sound onset. Error bars: SE. *B*: examinations of the correlation in the neural fragment detection index (FDI) between the BIC-stimulation condition and the Corgap-stimulation condition for the FFR_{TFS} (*left*) and the FFR_{Env} (*right*).

B

To test whether the FDI under the BIC-stimulation condition and that under the Corgap-stimulation condition shared a common neural mechanism, Pearson correlation tests for FDI between the two conditions were conducted for FFR_{TFS} and FFR_{Env}, separately. As shown in Fig. 3*B*, no significant correlation was found between the two stimulation conditions for either FFR_{TFS} or FFR_{Env}.

To compare the effect of introduction of a BIC or a Corgap on the FFR_{TFS} and on the FFR_{Env}, the FFR_{TFS}-FFR_{Env} FDI matrix was examined, in which FFR_{TFS} was presented on the *y*-axis and FFR_{Env} was presented on the *x*-axis (Fig. 4). As shown in Fig. 4, the majority of the BIC FFR_{TFS} FDIs were larger than the BIC FFR_{Env} FDIs (most filled circles are above the diagonal). However, this pattern was not present for Corgap FDIs.

DISCUSSION

This study showed that a steady-state narrowband noise can elicit remarkable FFRs in the auditory midbrain IC, which is the end point integrating inputs from lower auditory brain stem structures for binaural processing (Li and Kelly 1992; Palmer et al. 1999; Shackleton et al. 2005; Shackleton and Palmer 2006; Yin et al. 1987). Since FFRs are based on precisely phase-locked responses of neuron populations to instantaneous waveforms of acoustic stimuli (Chandrasekaran and Kraus 2010; Du et al. 2009a, 2009b, 2011, 2012; Marsh and Worden 1969; Moushegian et al. 1973; Ping et al. 2008; Weinberger et al. 1970; Worden and Marsh 1968), narrowband noises are

useful for investigating phase locking-based neural mechanisms underlying binaural integration.

Moreover, the noise-evoked FFRs exhibit two temporal components: the fast-varying FFR_{TFS} signaling the center frequency and the slow-varying FFR_{Env} signaling the bandwidth. Thus the FFR_{TFS} and FFR_{Env} precisely represent the spectral
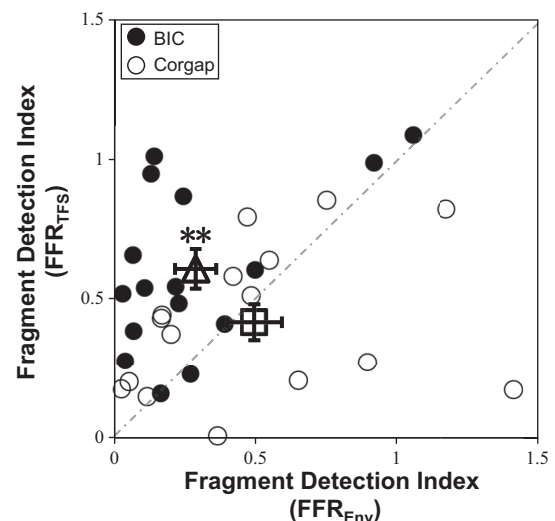

Fig. 4. Examination of the correlation in FDI between the FFR_{TFS} and the FFR_{Env} under the BIC-stimulation condition and under the Corgap-stimulation condition. Note that under the BIC-stimulation condition most of the FFR_{TFS} FDIs were larger than FFR_{Env} FDIs (black dots). Triangle, mean of BIC FDIs; square, mean of Corgap FDIs. Error bars: SE. **$P < 0.01$.

features of a narrowband noise. The results support the concept that FFRs efficiently convey both TFS information (e.g., Chandrasekaran and Kraus 2010; Du et al. 2011; Galbraith 1994; Krishnan 2002; Krishnan and Gandour 2009; Russo et al. 2004) and envelope information (also called envelope-following response) (e.g., Aiken and Picton 2006, 2008; Dolphin and Mountain 1992, 1993; Hall 1979; Shinn-Cunningham et al. 2013; Supin and Popov 1995; Zhu et al. 2013).

More importantly, this study for the first time provides evidence showing that introduction of a BIC reduces both the FFR_{TFS} and FFR_{Env}. Since introducing a BIC does not substantially change monaural inputs, the FFR reduction must be based on binaural interactions, which have been demonstrated previously (Du et al. 2009b). The BIC-induced FFR reduction may be the neural correlate underlying perceptual detection of the BIC (Akeroyd and Summerfield 1999; Boehnke et al. 2002; Huang et al. 2008, 2009a, 2009b; Kong et al. 2012, 2015; Li et al. 2009, 2013).

When the FDI is used to estimate the degree of FFR changes caused by introducing a fragment (BIC or Corgap), the BIC-induced FDI for FFR_{TFS} is larger than that for FFR_{Env}, indicating that introduction of a BIC causes more reduction in FFR_{TFS} than in FFR_{Env}. The Boehnke et al. (2002) study showed that the envelope information is not as important as the TFS information in determining the detection of the BIC detection. Clearly, further perceptual work is needed to verify whether the processing of FFR_{TFS} contributes more to the BIC detection than the processing of FFR_{Env}. However, the Corgap-induced FDI for FFR_{TFS} is not significantly different from that for FFR_{Env}. Since IAC-based binaural processing plays a role in both sound localization (Coffey et al. 2006; Franken et al. 2014; Soeta and Nakagawa 2006) and target-object detection against masking (Durlach et al. 1986; Palmer et al. 1999), further perceptual work is also needed to verify whether FFR_{TFS} signals are more involved in sound localization and target unmasking than FFR_{Env} signals. Smith et al. (2002) have suggested that TFS signals and envelope signals are most important for pitch/location perception and speech recognition, respectively. It is of interest to know whether this functional dichotomy between TFS and envelope is associated with certain differences in sensitivity to the BIC between FFR_{TFS} and FFR_{Env}.

The IC is the end point converging inputs from lower auditory brain stem structures (Palmer et al. 1999; Shackleton et al. 2005; Shackleton and Palmer 2006; Yin et al. 1987). Previous studies have suggested that binaural integration occurs in the IC (Du et al. 2009b; Kelly and Li 1997; Li and Kelly 1992). Does the IAC-based binaural integration follow a simple linear summation (cross-correlation) function? The results of this study indicate that for either FFR_{TFS} or FFR_{Env} the BIC-induced FDI is independent of the Corgap-induced FDI. Thus the BIC-induced changes in FFRs cannot be explained by a simple signal input reduction.

Summary. In the IC, a narrowband noise can efficiently induce FFRs that contain both the FFR_{TFS} and FFR_{Env} components, signaling the center frequency and bandwidth, respectively. Introduction of a BIC reduces both FFR_{TFS} and FFR_{Env}, and the FFR reductions cannot be explained by a simple reduction in linear summation of signal inputs from the two ears.

AUTHOR CONTRIBUTIONS

Author contributions: Q.W. and L.L. conception and design of research; Q.W. performed experiments; Q.W. analyzed data; Q.W. and L.L. interpreted results of experiments; Q.W. prepared figures; Q.W. and L.L. drafted manuscript; Q.W. and L.L. edited and revised manuscript; Q.W. and L.L. approved final version of manuscript.

REFERENCES

Aiken SJ, Picton TW. Envelope following responses to natural vowels. *Audiol Neurootol* 11: 213–232, 2006.

Aiken SJ, Picton TW. Envelope and spectral frequency-following responses to vowel sounds. *Hear Res* 245: 35–47, 2008.

Akeroyd MA, Summerfield AQ. A binaural analog of gap detection. *J Acoust Soc Am* 105: 2807–2820, 1999.

Blauert J, Lindemann W. Spatial mapping of intracranial auditory events for various degrees of interaural coherence. *J Acoust Soc Am* 79: 806–813, 1986.

Boehnke SE, Hall SE, Marquardt T. Detection of static and dynamic changes in interaural correlation. *J Acoust Soc Am* 112: 1617–1626, 2002.

Burkard R. Human brain-stem auditory evoked responses obtained by cross correlation to trains of clicks, noise bursts, and tone bursts. *J Acoust Soc Am* 90: 1398–1404, 1991.

Chandrasekaran B, Kraus N. The scalp-recorded brainstem response to speech: neural origins and plasticity. *Psychophysiology* 47: 236–246, 2010.

Coffey CS, Ebert CS, Marshall AF, Skaggs JD, Falk SE, Crocker WD, Pearson JM, Fitzpatrick DC. Detection of interaural correlation by neurons in the superior olivary complex, inferior colliculus and auditory cortex of the unanesthetized rabbit. *Hear Res* 221: 1–16, 2006.

Culling JF, Colburn HS, Spurchise M. Interaural correlation sensitivity. *J Acoust Soc Am* 110: 1020–1029, 2001.

Dau T. The importance of cochlear processing for the formation of auditory brainstem and frequency following responses. *J Acoust Soc Am* 113, 936–950, 2003.

Dobie RA, Wilson MJ. Short-latency auditory responses obtained by cross correlation. *J Acoust Soc Am* 76: 1411–1421, 1984.

Dolphin WF, Mountain DC. The envelope following response: scalp potentials elicited in the Mongolian gerbil using sinusoidally AM acoustic signals. *Hear Res* 58: 70–78, 1992.

Dolphin WF, Mountain DC. The envelope following response (EFR) in the Mongolian gerbil to sinusoidally amplitude-modulated signals in the presence of simultaneously gated pure tones. *J Acoust Soc Am* 94: 3215–3226, 1993.

Du Y, Huang Q, Wu XH, Galbraith GC, Li L. Binaural unmasking of frequency-following responses in rat amygdala. *J Neurophysiol* 101: 1647–1659, 2009a.

Du Y, Kong LZ, Wang Q, Wu XH, Li L. Auditory frequency-following response: a neurophysiological measure for studying the "cocktail-party problem." *Neurosci Biobehav Rev* 35: 2046–2057, 2011.

Du Y, Ma TF, Wang Q, Wu XH, Li L. Two crossed axonal projections contribute to binaural unmasking of frequency-following responses in rat inferior colliculus. *Eur J Neurosci* 30: 1779–1789, 2009b.

Du Y, Wang Q, Zhang Y, Wu XH, Li L. Perceived target-masker separation unmasks responses of lateral amygdala to the emotionally conditioned target sounds in awake rats. *Neuroscience* 225: 249–257, 2012.

Durlach NI, Gabriel KJ, Colburn HS, Trahiotis C. Interaural correlation discrimination. II. Relation to binaural unmasking. *J Acoust Soc Am* 79: 1548–1557, 1986.

Fitzpatrick DC, Roberts JM, Kuwada S, Kim DO, Filipovic B. Processing temporal modulations in binaural and monaural auditory stimuli by neurons in the inferior colliculus and auditory cortex. *J Assoc Res Otolaryngol* 10: 579–593, 2009.

Franken TP, Bremen P, Joris PX. Coincidence detection in the medial superior olive: mechanistic implications of an analysis of input spiking patterns. *Front Neural Circuits* 8: 42, 2014.

Galbraith GC. Two-channel brain-stem frequency-following responses to pure tone and missing fundamental stimuli. *Electroencephalogr Clin Neurophysiol* 92: 321–330, 1994.

Gnansia D, Pe'an V, Meyer B, Lorenzi C. Effects of spectral smearing and temporal fine structure degradation on speech masking release. *J Acoust Soc Am* 125: 4023–4033, 2009.

Hall JW. Auditory brainstem frequency following responses to waveform envelope periodicity. *Science* 205: 1297–1299, 1979.

Hopkins K, Moore BC. The contribution of temporal fine structure to the intelligibility of speech in steady and modulated noise. *J Acoust Soc Am* 125: 442–446, 2009.

Huang Y, Huang Q, Chen X, Wu XH, Li L. Transient auditory storage of acoustic details is associated with release of speech from informational masking in reverberant conditions. *J Exp Psychol Hum Percept Perform* 35: 1618–1628, 2009a.

Huang Y, Kong LZ, Fan SL, Wu XH, Li L. Both frequency and interaural delay affect event-related potential responses to binaural gap. *Neuroreport* 19: 1673–1678, 2008.

Huang Y, Li JY, Zou XF, Qu TS, Wu XH, Mao LH, Wu YH, Li L. Perceptual fusion tendency of speech sounds. *J Cogn Neurosci* 23: 1003–1014, 2011.

Huang Y, Wu XH, Li L. Detection of the break in interaural correlation is affected by interaural delay, aging, and center frequency. *J Acoust Soc Am* 126: 300–309, 2009b.

Jeffress LA, Blodgett HC, Deatherage BH. Effect of interaural correlation on the precision of centering a noise. *J Acoust Soc Am* 34: 1122–1123, 1962.

Johnson DH. The relationship between spike rate and synchrony in responses of auditory-nerve fibers to single tones. *J Acoust Soc Am* 68: 1115–1122, 1980.

Joris PX, Yin TC. Responses to amplitude-modulated tones in the auditory nerve of the cat. *J Acoust Soc Am* 91: 215–232, 1992.

Kelly JB, Li L. Two sources of inhibition affecting binaural evoked responses in the rat's inferior colliculus: the dorsal nucleus of the lateral lemniscus and the superior olivary complex. *Hear Res* 104: 112–126, 1997.

Kong LZ, Xie ZL, Lu LX, Qu TS, Wu XH, Yan J, Li L. Similar impacts of the interaural delay and interaural correlation on binaural gap detection. *PLoS One* 10: e0126342, 2015.

Kong LZ, Xie ZL, Lu LX, Wu XH, Li L. Sensitivity to a break in interaural correlation is co-modulated by intensity level and interaural delay. *J Acoust Soc Am* 132: EL114–EL118, 2012.

Krishnan A. Human frequency-following responses: representation of steady-state synthetic vowels. *Hear Res* 166: 192–201, 2002.

Krishnan A, Gandour JT. The role of the auditory brainstem in processing linguistically-relevant pitch patterns. *Brain Lang* 10: 135–146, 2009.

Kuokkanen PT, Wagner H, Ashida G, Carr CE, Kempter R. On the origin of the extracellular field potential in the nucleus laminaris of the barn owl (*Tyto alba*). *J Neurophysiol* 104: 2274–2290, 2010.

Li HH, Kong LZ, Wu XH, Li L. Primitive auditory memory is correlated with spatial unmasking that is based on direct-reflection integration. *PLoS One* 8: e63106, 2013.

Li L, Huang J, Wu XH, Qi JG, Schneider BA. The effects of aging and interaural delay on the detection of a break in the interaural correlation between two sounds. *Ear Hear* 30: 273–286, 2009.

Li L, Kelly JB. Inhibitory influence of the dorsal nucleus of the lateral lemniscus on binaural responses in the rat's inferior colliculus. *J Neurosci* 12: 4530–4539, 1992.

Longtin A, Middleton JW, Cieniak J, Maler L. Neural dynamics of envelope coding. *Math Biosci* 214: 87–99, 2008.

Marsh JT. Differential brainstem pathways for the conduction of auditory frequency-following responses. *Electroencephalogr Clin Neurophysiol* 36: 415–424, 1974.

Marsh JT, Worden FG. Some factors modulating neural activities in peripheral auditory centers. *Brain Res* 12: 99–111, 1969.

Moon IJ, Won JH, Park MH, Ives DT, Nie K, Heinz MG, Lorenzi C, Rubinstein JT. Optimal combination of neural temporal envelope and fine structure cues to explain speech identification in background noise. *J Neurosci* 34: 12145–12154, 2014.

Moore BC. The role of temporal fine structure processing in pitch perception, masking, and speech perception for normal-hearing and hearing-impaired people. *J Assoc Res Otolaryngol* 9: 399–406, 2008.

Moushegian G, Rupert AL, Stillman RD. Scalp-recorded early responses in man to frequencies in the speech range. *Electroencephalogr Clin Neurophysiol* 35: 665–667, 1973.

Palmer AR, Jiang D, McAlpine D. Desynchronizing responses to correlated noise: a mechanism for binaural masking level differences at the inferior colliculus. *J Neurophysiol* 81: 722–734, 1999.

Paxinos G, Watson C. *The Rat Brain in Stereotaxic Coordinates* (3rd ed.). London: Academic, 1997.

Ping JL, Li NX, Galbraith GC, Wu XH, Li L. Auditory frequency-following responses in rat ipsilateral inferior colliculus. *Neuroreport* 19: 1377–1380, 2008.

Rosen S. Temporal information in speech: acoustic, auditory and linguistic aspects. *Philos Trans R Soc Lond B Biol Sci* 336: 367–373, 1992.

Russo N, Nicol T, Musacchia G, Kraus N. Brainstem responses to speech syllables. *Clin Neurophysiol* 115: 2021–2030, 2004.

Shackleton TM, Arnott RH, Palmer AR. Sensitivity to interaural correlation of single neurons in the inferior colliculus of guinea pigs. *J Assoc Res Otolaryngol* 6: 244–259, 2005.

Shackleton TM, Palmer AR. Contributions of intrinsic neural and stimulus variance to binaural sensitivity. *J Assoc Res Otolaryngol* 7: 425–442, 2006.

Shinn-Cunningham B, Ruggles DR, Bharadwaj H. How early aging and environment interact in everyday listening: from brainstem to behavior through modeling. In: *Basic Aspects of Hearing: Physiology and Perception*. New York: Springer, 2013, p. 501–510.

Smith JC, Marsh JT, Brown WS. Far-field recorded frequency-following responses: evidence for the locus of brainstem sources. *Electroencephalogr Clin Neurophysiol* 39: 465–472, 1975.

Smith ZM, Delgutte B, Oxenham AJ. Chimaeric sounds reveal dichotomies in auditory perception. *Nature* 416: 87–90, 2002.

Soeta Y, Nakagawa S. Auditory evoked magnetic fields in relation to interaural time delay and interaural correlation. *Hear Res* 220: 106–115, 2006.

Sohmer H, Pratt H, Kinarti R. Sources of frequency following responses (FFR) in man. *Electroencephalogr Clin Neurophysiol* 42: 656–664, 1977.

Supin AY, Popov VV. Envelope-following response and modulation transfer function in the dolphin's auditory system. *Hear Res* 92: 38–46, 1995.

Wagner H, Brill S, Kempter R, Carr CE. Microsecond precision of phase delay in the auditory system of the barn owl. *J Neurophysiol* 94: 1655–1658, 2005.

Wagner H, Brill S, Kempter R, Carr CE. Auditory responses in the barn owl's nucleus laminaris to clicks: impulse response and signal analysis of neurophonic potential. *J Neurophysiol* 102: 1227–1240, 2009.

Weinberger NM, Kitzes LM, Goodman DA. Some characteristics of the "auditory neurophonic." *Experientia* 26: 46–48, 1970.

Worden FG, Marsh JT. Frequency-following (microphonic-like) neural responses evoked by sound. *Electroencephalogr Clin Neurophysiol* 25: 42–52, 1968.

Yin TC, Chan JC, Carney LH. Effects of interaural time delays of noise stimuli on low-frequency cells in the cat's inferior colliculus. III. Evidence for cross-correlation. *J Neurophysiol* 58: 562–583, 1987.

Young ED, Sachs MB. Representation of steady-state vowels in the temporal aspects of the discharge patterns of populations of auditory-nerve fibers. *J Acoust Soc Am* 66: 1381–1403, 1979.

Zhu L, Bharadwaj H, Xia J, Shinn-Cunningham B. A comparison of spectral magnitude and phase-locking value analyses of the frequency-following response to complex tones. *J Acoust Soc Am* 134: 384–395, 2013.